รายงานวิจัยฉบับสมบูรณ์

โครงการ การพัฒนาตัวควบคุมไมโครอิเล็กทรอนิกส์ซึ่งมีการฝังด้วยวิธีการใหม่ของการควบคุมเชิงทำนายแบบจำลองคงทนที่มีพื้นฐานเป็นท่อป้อนกลับผลลัพธ์แบบไม่เชื่อมตรงสำหรับกระบวนการเกิดพอลิเมอร์ที่มีความไม่แน่นอนร่วมกับความผิดพลาดของการประมาณสถานะ (MRG6180035)

โดย ผู้ช่วยศาสตราจารย์ ดร.พรชัย บำรุงศรี
รองศาสตราจารย์ ดร.สุรเทพ เขียวหอม

พฤษภาคม 2563

สัญญาเลขที่ MRG6180035

รายงานวิจัยฉบับสมบูรณ์

โครงการ การพัฒนาตัวควบคุมไมโครอิเล็กทรอนิกส์ซึ่งมีการฝังด้วยวิธีการใหม่ของการควบคุมเชิงทำนายแบบจำลองคงทนที่มีพื้นฐานเป็นท่อป้อนกลับผลลัพธ์แบบไม่เชื่อมตรงสำหรับกระบวนการเกิดพอลิเมอร์ที่มีความไม่แน่นอนร่วมกับความผิดพลาดของการประมาณสถานะ (MRG6180035)

ผู้ช่วยศาสตราจารย์ ดร.พรชัย บำรุงศรี มหาวิทยาลัยมหิดล
รองศาสตราจารย์ ดร.สุรเทพ เขียวหอม จุฬาลงกรณ์มหาวิทยาลัย

สนับสนุนโดยสำนักงานคณะกรรมการการอุดมศึกษา และสำนักงานกองทุนสนับสนุนการวิจัย

สารบัญ

บทคัดย่อ

รหัสโครงการ: MRG6180035

ชื่อโครงการ: การพัฒนาตัวควบคุมไมโครอิเล็กทรอนิกส์ซึ่งมีการฝังด้วยวิธีการใหม่ของการควบคุมเชิงทำนายแบบจำลองคงทนที่มีพื้นฐานเป็นท่อป้อนกลับผลลัพธ์แบบไม่เชื่อมตรงสำหรับกระบวนการเกิดพอลิเมอร์ที่มีความไม่แน่นอนร่วมกับความผิดพลาดของการประมาณสถานะ

ชื่อนักวิจัย และสถาบัน: ผศ.ดร.พรชัย บำรุงศรี มหาวิทยาลัยมหิดล
รศ.ดร.สุรเทพ เขียวหอม จุฬาลงกรณ์มหาวิทยาลัย

อีเมล์: pornchai.bum@mahidol.ac.th, soorathep.k@chula.ac.th

ระยะเวลาโครงการ: 2 พฤษภาคม 2561 ถึง 1 พฤษภาคม 2563

งานวิจัยนี้ได้ทำการพัฒนาวิธีการใหม่ของการควบคุมเชิงทำนายแบบจำลองคงทนซึ่งสามารถรับประกันเสถียรภาพความคงทนของระบบภายใต้อิทธิพลของพารามิเตอร์ที่มีความไม่แน่นอน ตัวแปรรบกวน และสัญญาณรบกวนของการวัด วิธีการควบคุมเชิงทำนายแบบจำลองคงทนที่พัฒนาขึ้นสามารถจำกัดขอบเขตผลกระทบของความไม่แน่นอนทั้งหมดและความผิดพลาดของการประมาณสถานะให้อยู่ภายในบริเวณของท่อยืนยงจึงสามารถลดผลกระทบของความไม่แน่นอนได้อย่างมีนัยสำคัญ นอกจากนี้ได้ทำการแก้ไขปัญหาการหาค่าเหมาะสมที่สุดก่อนและกฎการควบคุมสามารถฝังตัวลงในตัวควบคุมไมโครอิเล็กทรอนิกส์จึงสามารถนำไปประยุกต์ใช้กับการควบคุมระบบที่มีพลวัตรวดเร็วได้ เมื่อทำการเปรียบเทียบกับวิธีการควบคุมเชิงทำนายแบบจำลองคงทนดั้งเดิมพบว่าวิธีการควบคุมเชิงทำนายแบบจำลองคงทนที่พัฒนาขึ้นสามารถให้สมรรถนะการควบคุมที่ดีกว่าและใช้เวลาการคำนวณที่น้อยกว่า ในขั้นตอนสุดท้ายได้มีการนำวิธีการควบคุมเชิงทำนายแบบจำลองคงทนที่พัฒนาขึ้นไปประยุกต์ใช้กับการควบคุมถังปฏิกรณ์ฟลูอิไดซ์เบดขนาดนำร่องสำหรับพอลิเอทิลีนความหนาแน่นต่ำ โดยอนุภาคของพอลิเอทิลีนความหนาแน่นต่ำจะถูกบรรจุในหอซึ่งมีการสร้างความร้อนภายในเบดของอนุภาคตามกฎอัตราของการเกิดพอลิเมอร์ซึ่งคำนวณด้วยคอมพิวเตอร์ ภายใต้อิทธิพลของความไม่แน่นอนในกระบวนการ เช่น ค่าคงที่อัตราของปฏิกิริยา ค่าความร้อนของปฏิกิริยา ตัวแปรรบกวน และสัญญาณรบกวนของการวัด พบว่าวิธีการใหม่ของการควบคุมเชิงทำนายแบบจำลองคงทนที่พัฒนาขึ้นสามารถควบคุมอุณหภูมิของระบบให้เข้าสู่ค่าเป้าหมายจึงสามารถรับประกันเสถียรภาพความคงทนได้

คำหลัก: ตัวควบคุมไมโครอิเล็กทรอนิกส์ การควบคุมเชิงทำนายแบบจำลองคงทนที่มีพื้นฐานเป็นท่อป้อนกลับผลลัพธ์แบบไม่เชื่อมตรง กระบวนการพอลิเมอร์ที่มีความไม่แน่นอน ความผิดพลาดของการประมาณสถานะ เสถียรภาพคงทน

Abstract

Project Code: MRG6180035

Project Title: Development of a microelectronic controller embedded with novel off-line output feedback tube-based robust model predictive control for uncertain polymerization processes with state estimation errors

Investigator: Asst. Prof. Dr. Pornchai Bumroongsri Mahidol University

Assoc. Prof. Dr. Soorathep Kheawhom Chulalongkorn University

E-mail Address: pornchai.bum@mahidol.ac.th, soorathep.k@chula.ac.th

Project Period: 2th May, 2018 to 1st May, 2020 (2 years)

This research develops a novel robust model predictive control algorithm that can guarantee robust stability of the systems under the influences of uncertain parameters, disturbances and measurement noises. The developed robust model predictive control algorithm can bound the effects of all uncertainties and state estimation errors in the regions of invariant tubes so the effects of uncertainties can be significantly reduced. In addition, the optimization problem is solved off-line and the control law can be embedded in the microelectronic controller so it can be applied to the control of fast dynamical systems. As compared with the conventional robust model predictive control algorithm, the developed robust model predictive control algorithm can give better control performance and use less computational time. In the last step, the developed robust model predictive control algorithm is applied to the control of a pilot-scale fluidized bed reactor for low-density polyethylene (LDPE). The LDPE particles are loaded into the chamber that generates heat in the bed of particles according to the rate law of polymerization calculated by the computer. Under the influences of uncertainties in the process such as the reaction rate constant, heat of reaction, disturbances and measurement noises, the developed robust model predictive control algorithm can regulate the temperature of the system to the set point so robust stability can be guaranteed.

Keywords: Microelectronic controller; off-line output feedback tube-based robust model predictive control; uncertain polymerization processes; state estimation errors; robust stability

1. Executive summary

The control of the industrial processes when not all states can be exactly measurable is a challenging control problem because it is difficult to ensure both robust stability and constraint satisfaction as the state estimator is employed. Additionally, this problem is more severe in the case when there are some uncertain parameters and disturbances present in the process due to the mismatch between the real process and the process model. In order to efficiently control the uncertain industrial processes, it is important to develop an advanced control algorithm that can handle the effects of state estimation errors and all possible sources of uncertainties including the uncertain parameters, disturbances and measurement noises

In this research, a novel off-line output feedback tube-based robust model predictive control algorithm is developed. The effects of the state estimation errors and all possible sources of uncertainties including the uncertain parameters, disturbances and measurement noises are bounded within the tubes so robust stability and constraint satisfaction can be guaranteed. All optimization problems are solved off-line to find the explicit control laws for on-line applications. These explicit control laws can be embedded into a microelectronic controller so it can be used for fast dynamical systems. As compared with the conventional model predictive controller in the literature, the proposed controller can achieve better control performance and lower computational time. The obtained results have contributed to the development of the advanced process control theory because a novel control algorithm has been developed in this research.

The developed controller is applied to a challenging control problem of a pilot-scale fluidized bed reactor for low-density polyethylene (LDPE). The LDPE particles are loaded into the pilot-scale fluidized bed reactor and the heat within the particle bed is generated according to the uncertain rate law of polymerization simulated from the computer. The developed robust model predictive control algorithm can regulate the temperature of the system to the set point so robust stability can be guaranteed. This pilot-scale reactor can be used as a prototype in the research and education of all process and chemical engineers.

2. Objectives of this research

(1) To develop a microelectronic controller embedded with novel off-line output feedback tube-based robust MPC algorithm that can guarantee robust stability and constraint satisfaction of the control systems in the presence of the state estimation errors and all possible sources of uncertainties including the uncertain parameters, disturbances and measurement noises.

(2) To develop a pilot-scale fluidized bed reactor for low-density polyethylene (LDPE). The heat within the particle bed is generated from the heater according to the uncertain rate law of polymerization simulated from the computer.

(3) To apply the developed microelectronic controller to the control of a pilot-scale fluidized bed reactor for low-density polyethylene (LDPE). Both robust stability and constraint satisfaction of the system are guaranteed despite the presence of state estimation errors and the sources of uncertainties such as uncertain reaction rate constant, uncertain heat of polymerization, measurement noises and disturbances.

3. Research Methodology

In this project, a microelectronic controller embedded with a novel off-line output feedback tube-based robust MPC algorithm is proposed. The proposed algorithm can handle uncertain parameters, disturbances, measurement noises and state estimation errors. Additionally, all of the optimization problems are solved off-line so the developed off-line tube-based robust MPC algorithm is applicable to fast dynamical processes. In order to illustrate its effectiveness, the proposed control algorithm will be applied to a pilot-scale fluidized bed polymerization reactor for low-density polyethylene (LDPE) production. The research methodology is shown in Fig. 3.1.

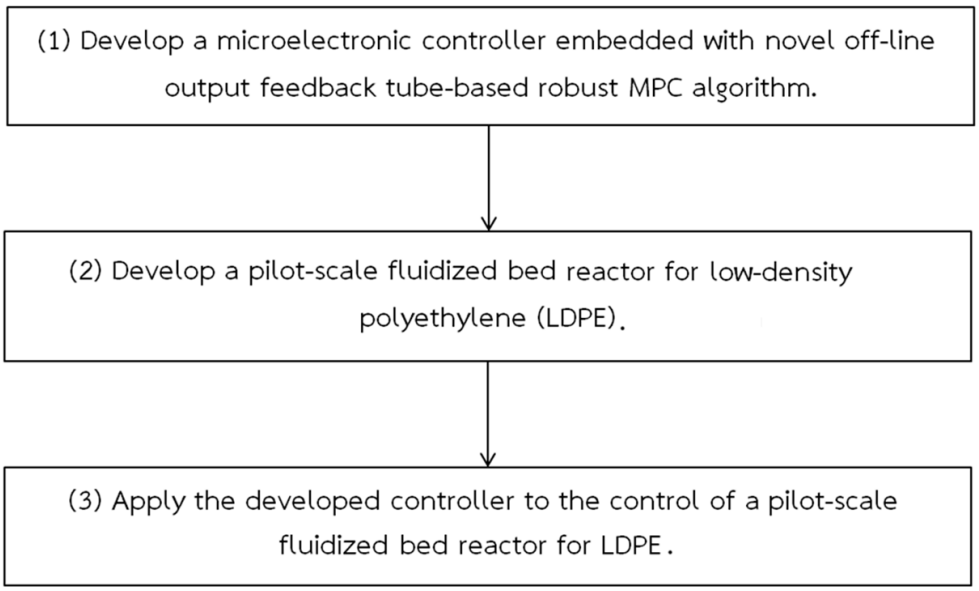

Figure 3.1 The research methodology.

(1) Develop a microelectronic controller embedded with novel off-line output feedback tube-based robust MPC algorithm.

A novel off-line output feedback tube-based robust MPC algorithm is developed. The explicit control laws are computed and can be embedded into a microelectronic controller so it can be conveniently and efficiently used for real-time

applications. Consider the following discrete-time system with uncertain parameter, bounded disturbance and measurement noise.

$$x^+ = A^\lambda x + B^\lambda u + w$$
$$y = C^\lambda x + v \tag{3.1}$$

where $x \in \mathbb{R}^n$ is the state that is not necessary to be measurable, $u \in \mathbb{R}^m$ is the control input, $w \in \mathbb{R}^n$ is the bounded disturbance, $x^+ \in \mathbb{R}^n$ is the successor state, $y \in \mathbb{R}^p$ is the measured output and $v \in \mathbb{R}^p$ is the measurement noise. The system is subject to the state constraint $x \in \mathbb{X}$ and the control constraint $u \in \mathbb{U}$ where $\mathbb{X} \subset \mathbb{R}^n$ and $\mathbb{U} \subset \mathbb{R}^m$ are compact, convex and each set contains the origin as an interior point. The state disturbance w and the measurement noise v are known only to the extent that they lie in, $w \in \mathbb{W}$ and $v \in \mathbb{V}$ where $\mathbb{W} \subset \mathbb{R}^n$ and $\mathbb{V} \subset \mathbb{R}^p$ are compact, convex and each set contains the origin as an interior point.

The matrices A^λ and B^λ are not constant but vary with an uncertain parameter vector λ. An uncertain parameter vector λ can be measured at each sampling time but its future values are uncertain. We make the following assumption

Assumption 1. $[A^\lambda \; B^\lambda \; C^\lambda] \in \mathrm{Conv}\{[A_1 \; B_1 \; C_1],...,[A_L \; B_L \; C_L]\}$ where Conv denotes the convex hull, $[A_j \; B_j \; C_j]$ are vertices of the convex hull and L is the number of vertices of the convex hull. Any $[A^\lambda \; B^\lambda \; C^\lambda]$ can be written as $[A^\lambda \; B^\lambda \; C^\lambda] = \sum_{j=1}^{L} \lambda_j [A_j \; B_j \; C_j]$. The pair $[A_j \; B_j]$ is controllable and the pair $[A_j \; C_j]$ is observable.

Since the state x is not necessary to be measurable, the following Luenberger observer is employed

$$\hat{x}^+ = A^\lambda \hat{x} + B^\lambda u + L(y - \hat{y})$$
$$\hat{y} = C^\lambda \hat{x} \tag{3.2}$$

where $\hat{x} \in \mathbb{R}^n$ is the observer state, $L \in \mathbb{R}^{nxp}$ is the observer gain, $\hat{y} \in \mathbb{R}^p$ is the observer output and $\hat{x}^+ \in \mathbb{R}^n$ is the observer successor state. Defining the state estimation error $\tilde{x}$ as $\tilde{x} = x - \hat{x}$, it is seen that

$$\tilde{x}^+ = (A^\lambda - LC^\lambda)\tilde{x} + (w - Lv). \tag{3.3}$$

The state estimation error will be bounded within a robust positively invariant set. The definition of the robust positively invariant set is as follows:

Definition 1. The set $Z \subset \mathbb{R}^n$ is a robust positively invariant set of an uncertain system with disturbance $x^+ = A^\lambda x + w$ if $A^\lambda Z \oplus \mathbb{W} \subseteq Z$ for $\forall x \in Z$, $\forall w \in \mathbb{W}$ and $\forall A^\lambda \in \text{Conv}\{A_1, ..., A_L\}$ where $\oplus$ denotes the Minkowski set addition (Mayne et al., 2009).

It can be observed that if L satisfies the Lyapunov stability constraint

$$(A_j - LC_j)^T P (A_j - LC_j) - P < 0, \forall j \in \{1, ..., L\} \tag{3.4}$$

where P is a Lyapunov matrix, then $(A^\lambda - LC^\lambda)^T P (A^\lambda - LC^\lambda) - P < 0$, $\forall [A^\lambda \; B^\lambda] \in \text{Conv}\{[A_j \; B_j], \forall j \in 1, 2, ..., L\}$ and we can bound the state estimation error $\tilde{x}$ by a robust positively invariant set $\tilde{S}$ satisfying

$$(A^\lambda - LC^\lambda)\tilde{S} \oplus \mathbb{W} \oplus (-L\,\mathbb{V}) \subseteq \tilde{S} \tag{3.5}$$

for $\forall (x - \hat{x}) \in \tilde{S}$, $\forall w \in \mathbb{W}$ and $\forall v \in \mathbb{V}$. The set $\tilde{S}$ can be approximated using the method in Raković et al. (2005).

Let the nominal system (system with no uncertain parameter, bounded disturbance and measurement noise) be defined by

$$\bar{x}^+ = A\bar{x} + B\bar{u} \tag{3.6}$$

where $\bar{x} \in \mathbb{R}^n$ is the state of the nominal system, $\bar{u} \in \mathbb{R}^m$ is the control input of the nominal system and $\bar{x}^+ \in \mathbb{R}^n$ is the successor state of the nominal system. We will control the observer state $\hat{x}$ in such a way that the state of the nominal system $\bar{x}$ converges to the target set. In order to counteract the effect of the uncertainty, the following control law is employed

$$u = \bar{u} + K(\hat{x} - \bar{x}) \tag{3.7}$$

where $K \in \mathbb{R}^{mxn}$ is the disturbance rejection gain. Defining the control error e as $e = \hat{x} - \bar{x}$, it is seen that

$$e^+ = (A + BK)e + LC^\lambda \tilde{x} + Lv + (A^\lambda - A)\hat{x} + (B^\lambda - B)u \tag{3.8}$$

It can be observed that if K satisfies the Lyapunov stability constraint

$$(A_j + B_j K)^T P(A_j + B_j K) - P < 0, \forall j \in \{1,...,L\} \tag{3.9}$$

where P is a Lyapunov matrix, then $(A^\lambda + B^\lambda K)^T P(A^\lambda + B^\lambda K) - P < 0$, $\forall [A^\lambda \; B^\lambda] \in \mathrm{Conv}\{[A_j \; B_j], \forall j \in 1,2,...,L\}$ and we can bound the control error e by a robust positively invariant set $\bar{S}$ satisfying

$$(A+BK)\bar{S} \oplus LC^\lambda \tilde{S} \oplus L\,\mathbb{V} \oplus (A^\lambda - A)\;\mathbb{X} \oplus (B^\lambda - B)\,\mathbb{U} \subseteq \bar{S} \tag{3.10}$$

for $\forall(\hat{x} - \bar{x}) \in \bar{S}$, $\forall(x - \hat{x}) \in \tilde{S}$, $\forall v \in \mathbb{V}$, $\forall x \in \mathbb{X}$ and $\forall u \in \mathbb{U}$. The set $\bar{S}$ can be approximated using the method in Raković et al. (2005).

Defining $S = \bar{S} \oplus \tilde{S}$, it is seen that if the state estimation error $\tilde{x} = x - \hat{x}$ satisfies $x - \hat{x} \in \tilde{S}$ and the control error $e = \hat{x} - \bar{x}$ satisfies $\hat{x} - \bar{x} \in \bar{S}$, then $x \in \hat{x} \oplus \tilde{S} \subseteq \bar{x} \oplus S$. For this reason, although the state x is not exactly known, we can control the observer state $\hat{x}$ in such a way that the unknown state x is bounded and the state of the nominal system $\bar{x}$ converges to the target set. In order to ensure that the unknown state x satisfies the state constraint $x \in \mathbb{X}$ and the control constraint $u \in \mathbb{U}$, we must

employ tighter constraints for the nominal system, i.e., $\bar{x} \in \mathbb{X} \ominus S$ and $\bar{u} \in \mathbb{U} \ominus K\bar{S}$. The optimization problem can be written as follows

$$\min_{\bar{x}_0, \bar{u}_k} \sum_{k=0}^{n-1} \left(\frac{1}{2}\right) (\bar{x}_k^T Q \bar{x}_k + \bar{u}_k^T R \bar{u}_k) + \left(\frac{1}{2}\right) \bar{x}_n^T P_f \bar{x}_n \tag{3.11}$$

$$\text{s.t. } \hat{x} \in \bar{x}_0 \oplus \bar{S} \tag{3.12}$$

$$\bar{x}_{k+1} = A\bar{x}_k + B\bar{u}_k, \ k \in \{0,\ldots,n-1\} \tag{3.13}$$

$$\bar{x}_k \in \mathbb{X} \ominus (\tilde{S} \oplus \bar{S}), \ \bar{u}_k \in \mathbb{U} \ominus K\bar{S}, \tag{3.14}$$

$$\bar{x}_n \in \bar{X}_f \tag{3.15}$$

where $\bar{x}_k$ and $\bar{u}_k$ are the predicted state and control input, respectively, in the prediction horizon n of the nominal system, Q, R and P_f are positive definite weighting matrices, $\bar{X}_f$ is the terminal constraint set and the Minkowski set addition and difference are defined, respectively, by $X \oplus Y := \{x + y \mid x \in X, y \in Y\}$ and $X \ominus Y := \{x \mid x \oplus Y \subseteq X\}$. In summary, the off-line output feedback tube-based robust MPC algorithm can be formulated as follows:

Step 1: Compute off-line a sequence of observer gains $L_i, i = 1,2,\ldots,N$ satisfying $(A_j - L_i C_j)^T P (A_j - L_i C_j) - P < 0, \forall j \in \{1,\ldots,L\}$ and a sequence of the disturbance rejection gain $K_i, i = 1,2,\ldots,N$ satisfying $(A_j + B_j K_i)^T P (A_j + B_j K_i) - P < 0, \forall j \in \{1,\ldots,L\}$.

Step 2: Compute off-line the corresponding sequence of robust positively invariant sets for state estimation error $\tilde{S}_i, i = 1,2,\ldots,N$ satisfying (3.5) and the corresponding sequence of robust positively invariant sets for control error $\bar{S}_i, i = 1,2,\ldots,N$ satisfying (3.10).

Step 3: Compute off-line the optimization problem (3.11)-(3.15) using the multi-parametric programming (Kvasnica et al., 2004) to find the control input of the nominal system $\bar{u}$ corresponding to the region of the state of the nominal system $\bar{x}$.

Step 4: All of the components in the control law have been explicitly computed off-line. Embed the pre-computed control law into the microelectronic controller for on-line utilization.

We can now establish our main Theorem as follows

Theorem 1: For any initial state x, observer state $\hat{x}$ and state of the nominal system $\bar{x}$ satisfying $\hat{x}-\bar{x}\in\bar{S}_i$ and $x-\hat{x}\in\tilde{S}_i$ where $\tilde{S}_i$ and $\bar{S}_i$ are the robust positively invariant sets for the state estimation error and the control error, respectively, in a sequence $i=1,2,...,N$, the proposed output feedback controller steers the initial observer state $\hat{x}$ and state x to the target sets $\bar{X}_f\oplus\bar{S}_i$ and $\bar{X}_f\oplus\bar{S}_i\oplus\tilde{S}_i$, respectively, while satisfying the state constraint $x\in\mathbb{X}$ and the control constraint $u\in\mathbb{U}$.

Proof:

Consider the difference equation for the control error $e^+=(A+BK)e+LC^{\lambda}\tilde{x}+Lv+(A^{\lambda}-A)\hat{x}+(B^{\lambda}-B)u$. The disturbance rejection gains $K_i, i=1,2,...,N$ have to satisfy the Lyapunov stability constraint $(A_j+B_jK_i)^T P(A_j+B_jK_i)-P<0,\forall j\in\{1,...,L\}$ so the control error $e=\hat{x}-\bar{x}$ is bounded by the robust positively invariant set $\bar{S}_i$. Consider the difference equation for the state estimation error $\tilde{x}^+=(A^{\lambda}-LC^{\lambda})\tilde{x}+(w-Lv)$. The observer gains $L_i, i=1,2,...,N$ satisfy the Lyapunov stability constraint $(A_j-L_iC_j)^T P(A_j-L_iC_j)-P<0,\forall j\in\{1,...,L\}$ so the state estimation error $\tilde{x}=x-\hat{x}$ is bounded by the robust positively invariant set $\tilde{S}_i$. From the optimal control problem (3.11)-(3.15), the state $\bar{x}$ of the nominal system must be driven to the terminal constraint $\bar{X}_f$. Since $\hat{x}-\bar{x}\in\bar{S}_i$ and $x-\hat{x}\in\tilde{S}_i$, the observer state $\hat{x}$ and the state x must be driven to the target sets $\bar{X}_f\oplus\bar{S}_i$ and $\bar{X}_f\oplus\bar{S}_i\oplus\tilde{S}_i$, respectively. The tighter constraints for the state and control input of the nominal system are employed in (3.14) so the state constraint $x\in\mathbb{X}$ and the input constraint $u\in\mathbb{U}$ are satisfied. □

(2) Develop a pilot-scale fluidized bed reactor for low-density polyethylene (LDPE).

Fluidized bed polymerization reactors are widely used in LDPE production process due to their several advantages such as high heat and mass transfer rate, simple construction and capability of continuous transport. However, the polymerization reaction occurring in the reactor is highly exothermic so the control of bed temperature is crucially important in order to avoid the runaway reactions especially in the presence of uncertain parameters such as uncertain reaction rate and uncertain heat of reaction. Moreover, the temperature measurement noises usually occur due to the fluctuating behavior in the fluidized bed reactor so the exact values of bed temperature are not explicitly known (Schneiderbauer et al., 2015; Li et al., 2016).

In this research, a pilot-scale fluidized bed polymerization reactor for LDPE production is developed. The LDPE particles are loaded within the fluidized bed reactor and the bed temperature is controlled using the developed microelectronic controller by adjusting the inlet air temperature fed to the bottom of the reactor. The heat in the particle bed is generated from the heater according to the uncertain rate law of polymerization. The uncertain polymerization reaction is simulated using the computer so there is no real polymerization reaction taking place in the reactor for the safety in experiments. The explicit control laws are embedded into a microelectronic controller so it can be conveniently and efficiently used for real-time applications.

(3) Apply the developed controller to the control of a pilot-scale fluidized bed reactor for LDPE.

In the last step, the developed robust model predictive control algorithm is applied to the control of a pilot-scale fluidized bed reactor for low-density polyethylene (LDPE). The uncertain polymerization reaction is simulated using the computer and the uncertain heat of reaction is generated from the heater according to the uncertain reaction rate. The control loop is shown in Figure 3.2.

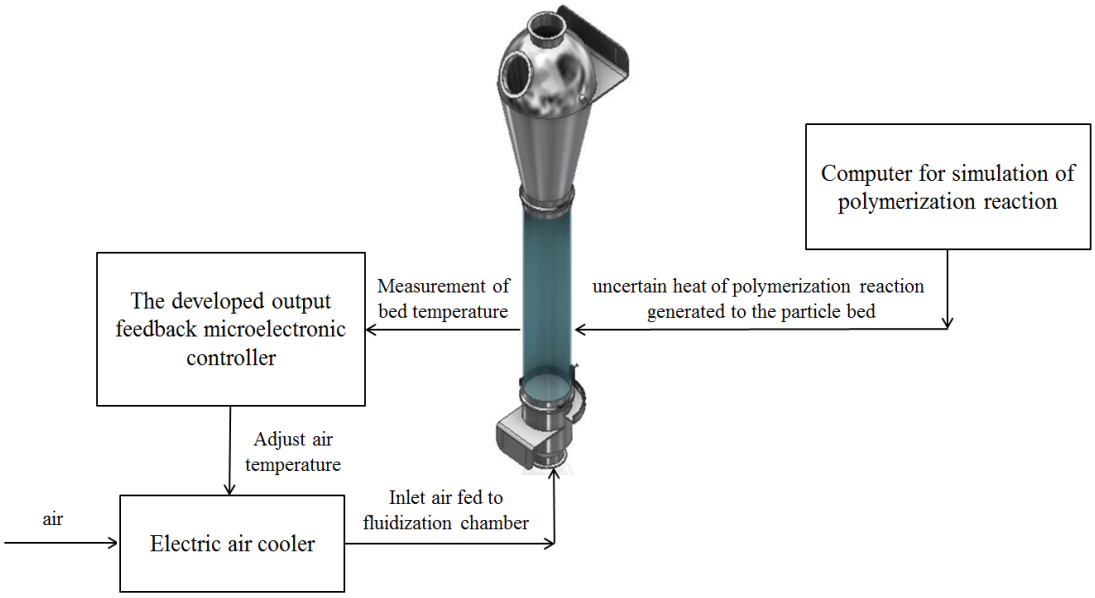

Figure 3.2 The control loop of a pilot-scale fluidized bed reactor.

The rate of polymerization reaction R_p simulated using the computer can be calculated as (Chen et al., 2011)

$$R_p = k_p \exp(-\frac{E}{RT})[M][C^*]. \tag{3.16}$$

The amount of heat generated from the polymerization Q_p can be calculated as

$$Q_p = R_p \Delta H \tag{3.17}$$

where $[M]$ is the simulated monomer concentration, $[C^*]$ is the simulated concentration of catalyst active site, T is the measured bed temperature, E is the activation energy and R is the gas constant.

Table 3.1 shows the uncertain parameters, measurement noises and disturbances occurring in the system. The reaction rate constant and the heat of polymerization are considered to be uncertain. The measurement noises usually occur due to the inherent fluctuating behavior in the fluidization so there exist the state estimation errors in the system.

Table 3.1 The uncertain parameters, measurement noises and disturbances.

Parameters	Descriptions	Nominal values	Units
K_p	reaction rate constant	10^6	$m^3mol^{-1}s^{-1}$
ΔH	heat of reaction	100	$kJmol^{-1}$
noises	Bed temperature measurement noises	± 0.1	K
disturbances	Inlet air temperature disturbances	± 0.2	K

The polymerization reaction is highly exothermic. In the presence of sources of uncertainty as shown in Table 3.1 and the state estimation errors, an inefficient control of the process may lead to unexpected thermal runaway of the system. For this reason, all possible sources of uncertainties and the state estimation errors are explicitly taken into account in the proposed output feedback controller.

4. Results of this research

(1) Results from the development of a microelectronic controller embedded with novel off-line output feedback tube-based robust MPC algorithm

Case study 1.1: Consider the following uncertain system with uncertain parameter, disturbance and measurement noise

$$x^+ = \begin{bmatrix} 1 & 1 \\ 0 & \lambda \end{bmatrix} x + \begin{bmatrix} 1 \\ 1 \end{bmatrix} u + w, \quad y = \begin{bmatrix} 1 & 0 \\ 0 & 1 \end{bmatrix} x + v. \tag{4.1}$$

The state constraint is $x \in \mathbb{X}$ where $\mathbb{X} := \{x \in \mathbb{R}^2 \mid [1\ 0]x \in [-50, 3], [0\ 1]x \in [-50, 3]\}$. The control constraint is $u \in \mathbb{U}$ where $\mathbb{U} := \{u \in \mathbb{R} \mid |u| \le 3\}$. The uncertain parameter is $\lambda \in \mathbb{L}$ where $\mathbb{L} := \{\lambda \in \mathbb{R} \mid 0.9 \le \lambda \le 1.1\}$. The disturbance and measurement noise are bounded $(w, v) \in \mathbb{W}\, x\, \mathbb{V}$ where $\mathbb{W} := \{w \in \mathbb{R}^2 \mid \|w\|_\infty \le 0.1\}$ and $\mathbb{V} := \{v \in \mathbb{R}^2 \mid \|v\|_\infty \le 0.01\}$. Since the state x is unmeasurable, the following Luenberger observer is employed

$$\hat{x}^+ = \begin{bmatrix} 1 & 1 \\ 0 & \lambda \end{bmatrix} \hat{x} + \begin{bmatrix} 1 \\ 1 \end{bmatrix} u + L_i(y - \hat{y}), \quad \hat{y} = C\hat{x} \tag{4.2}$$

where the observer gain L_i is updated at each sampling time. The nominal system is

$$\bar{x}^+ = \begin{bmatrix} 1 & 1 \\ 0 & 1 \end{bmatrix} \bar{x} + \begin{bmatrix} 1 \\ 1 \end{bmatrix} \bar{u}. \tag{4.3}$$

Figure 4.1 shows the robust positively invariant sets for the state estimation error $\tilde{S}_i, i = 1,2,...,5$. The robust positively invariant sets for the state estimation error $\tilde{S}_i$ are computed off-line.

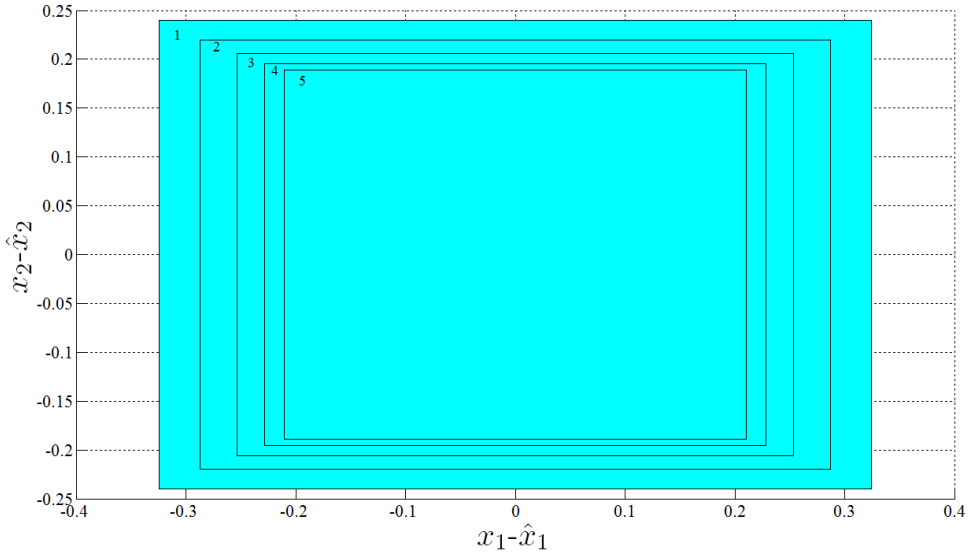

Figure 4.1 The robust positively invariant sets for the state estimation error $\widetilde{S}_i, i = 1,2,...,5$ computed off-line in case study 1.1.

Figure 4.2 shows the norm of the observer gains $\|L_i\|_2, i = 1,2,...,5$ corresponding to the robust positively invariant sets for the state estimation error $\widetilde{S}_i, i = 1,2,...,5$. The norm of the observer gains increases as i increases so larger value of the observer gain can be applied as the size of the robust positively invariant sets for the state estimation error decreases.

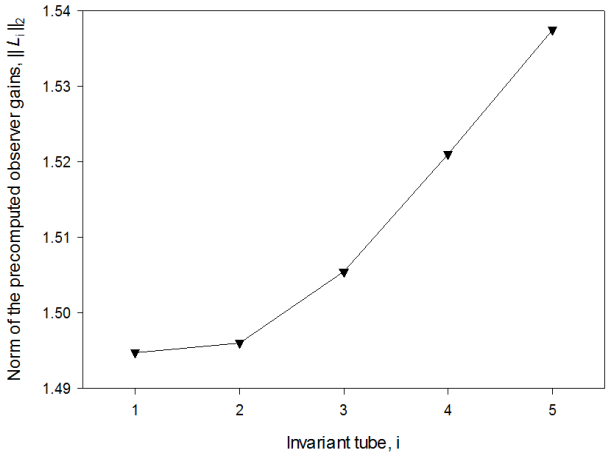

Figure 4.2 The norm of the observer gains $\|L_i\|_2, i = 1,2,...,5$ corresponding to the robust positively invariant sets for the state estimation error $\widetilde{S}_i, i = 1,2,...,5$.

Figure 4.3 shows the robust positively invariant sets for the control error $\overline{S}_i, i = 1,2,...,5$ computed off-line corresponding to the robust positively invariant sets for the state estimation error $\widetilde{S}_i, i = 1,2,...,5$.

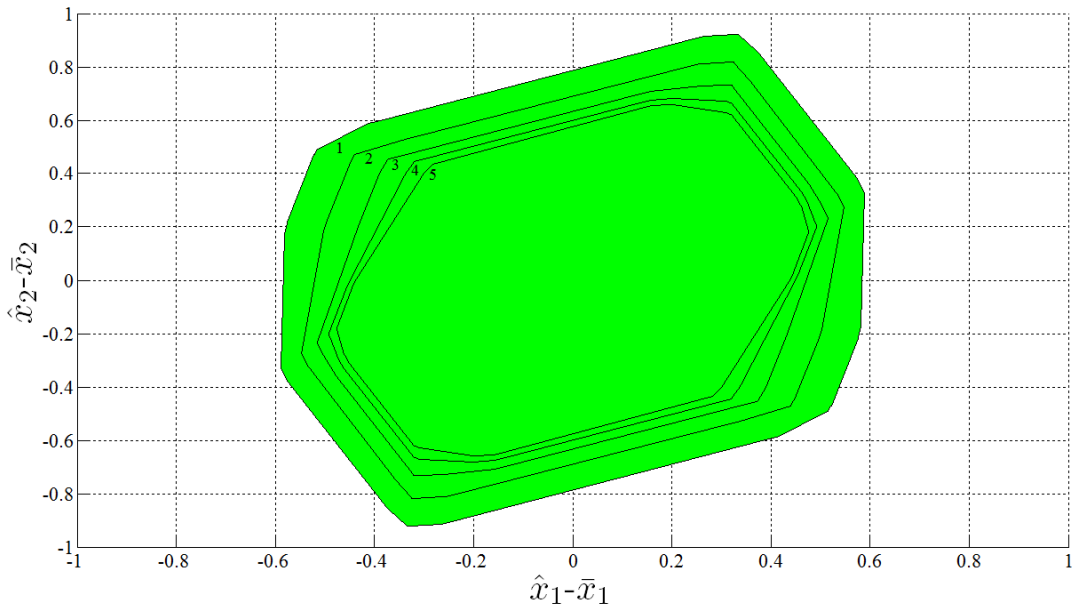

Figure 4.3 The invariant tubes for the control error $\overline{S}_i, i = 1,2,...,5$ computed off-line in case study 1.1.

Figure 4.4 shows the closed-loop responses of the systems. The invariant tubes for the state estimation error $\widetilde{S}_i$ and the control error $\overline{S}_i$ are shown in cyan and green, respectively. The yellow, red and blue lines represent the state trajectories of the uncertain system, the observer system and the nominal system, respectively. The target sets $\overline{X}_f$, $\overline{X}_f \oplus \overline{S}_i$ and $\overline{X}_f \oplus \overline{S}_i \oplus \widetilde{S}_i$ are shown in blue, red and yellow, respectively. The infeasible region for the state constraint is shown in magenta. Although the state x is unmeasurable, we can control the observer state $\hat{x}$ in such a way that the unknown state x is bounded and the state of the nominal system $\bar{x}$ converges to the target set.

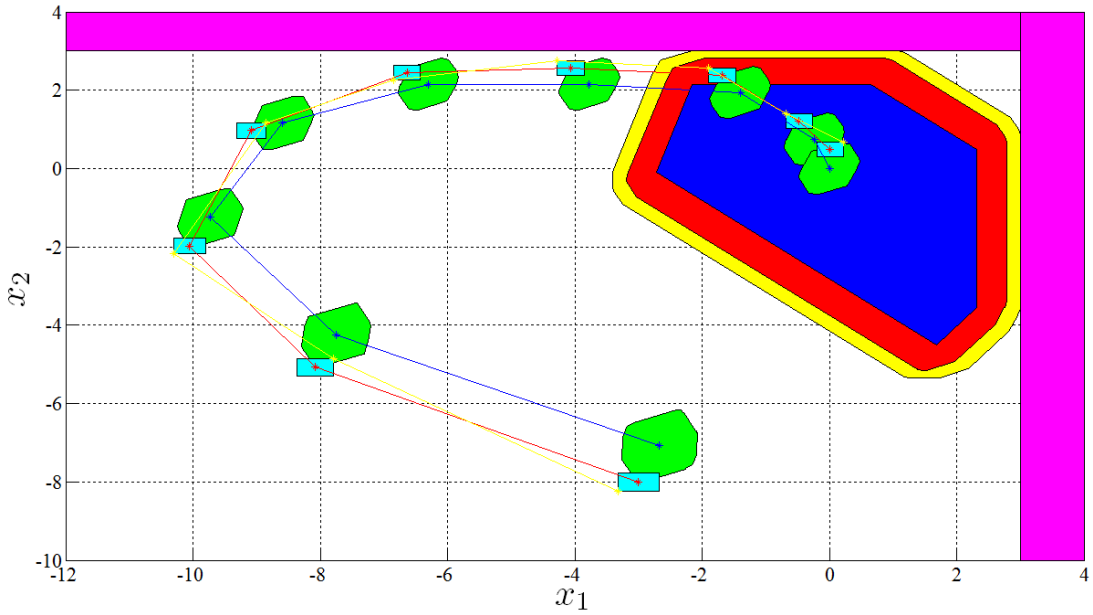

Figure 4.4 The closed-loop responses of the systems in case study 1.1. The invariant tubes for the state estimation error $\widetilde{S}_i$ and the control error $\overline{S}_i$ are shown in cyan and green, respectively. The yellow, red and blue lines represent the state trajectories of the uncertain system, the observer system and the nominal system, respectively. The target sets $\overline{X}_f$, $\overline{X}_f \oplus \overline{S}_i$ and $\overline{X}_f \oplus \overline{S}_i \oplus \widetilde{S}_i$ are shown in blue, red and yellow, respectively. The infeasible region for the state constraint is shown in magenta.

Figure 4.5 shows the control inputs of the systems. The control inputs of the nominal system and the uncertain system are represented by blue and red lines, respectively. The infeasible region for the input constraint is shown in yellow. The original constraint is satisfied by employing tighter constraint set for the nominal system.

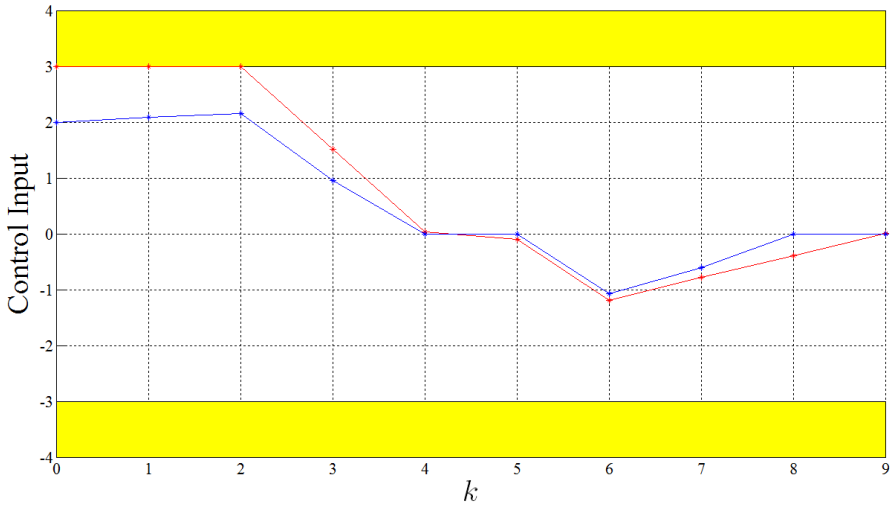

Figure 4.5 The control inputs of the systems. The control inputs of the nominal system and the uncertain system are represented by blue and red lines, respectively.

Table 4.1 shows the comparison between the proposed output feedback controller and the conventional output feedback tube-based controller (Mayne et al., 2006) where the observer gain, the robust positively invariant sets for the state estimation error and the robust positively invariant sets for the control error are constant for all time step. The proposed output feedback controller can achieve better performance cost $\sum_{k=1}^{\infty}(\bar{x}_k^T Q \bar{x}_k + \bar{u}_k^T R \bar{u}_k)$ due to the fact that the observer gain, the robust positively invariant sets for the state estimation error and the robust positively invariant sets for the control error can be updated. Note that $\bar{x}_k$ and $\bar{u}_k$ converge to the origin for large time step k. The on-line computational burden of the proposed output feedback controller is less than that required for the conventional output feedback tube-based controller. The computations are performed using Intel Core 2 Duo (2.53 GHz), 2 GB RAM.

Table 4.1 The comparison between the proposed output feedback controller and the conventional output feedback tube-based controller.

Algorithm	Performance Cost	On-line computational time per step (s)
The proposed algorithm	315.89	0.012
Mayne et al. (2006)	371.06	0.067

Figure 4.6 shows the domain of attraction (feasibility set for the optimal control problem with the prediction horizon $n=10$. The domain of attraction for the proposed output feedback controller is shown in blue and that of the conventional output feedback tube-based controller is shown in green. It is seen that the proposed output feedback controller has a larger domain of attraction compared with that of the conventional output feedback tube-based controller.

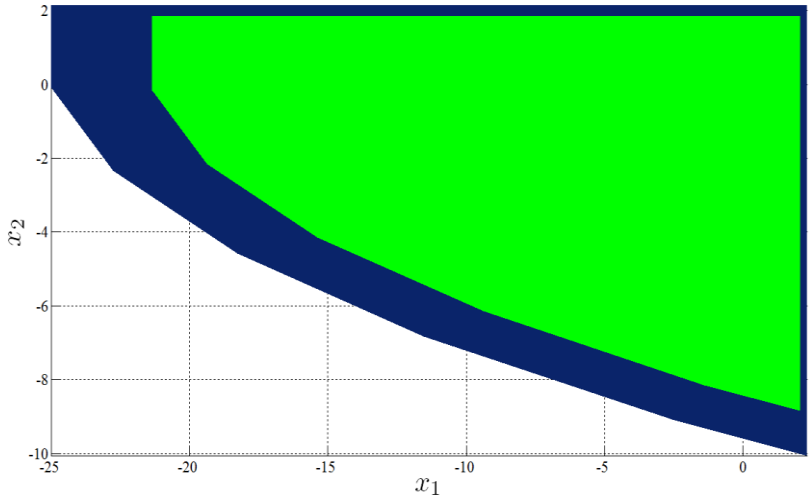

Figure 4.6 The domain of attraction. The domain of attraction for the proposed output feedback controller is shown in blue. The domain of attraction for the conventional output feedback tube-based controller (Mayne et al., 2006) is shown in green.

Case study 1.2: Consider the following uncertain model of a non-isothermal CSTR (Wan and Kothare, 2002)

$$x^+ = Ax + Bu + w\,,\;\; y = Cx + v \tag{4.4}$$

where x is a vector of the reactor concentration and temperature, u is the coolant flow, w is the state disturbance, y is a vector of measured output and v is the measurement noise. The system matrices can be written as

$$A = \begin{bmatrix} -\frac{F}{V} - k_o e^{-E/RT_S} & -\frac{E}{RT_s^2} k_o e^{-E/RT_S} C_{As} \\ \frac{-\Delta H_{rxn} k_o e^{-E/RT_S}}{\rho C_p} & -\frac{F}{V} - \frac{UA}{V\rho C_p} - \Delta H_{rxn} \frac{E}{\rho C_p RT_s^2} k_o e^{-E/RT_S} C_{As} \end{bmatrix},$$
$$B = \begin{bmatrix} 0 \\ -2.098x10^5 \frac{T_S - 365}{V\rho C_p} \end{bmatrix} \quad C = \begin{bmatrix} 1 & 0 \\ 0 & 1 \end{bmatrix} \tag{4.5}$$

where $F = 1\,\mathrm{m}^3/\mathrm{min}$, $V = 1\,\mathrm{m}^3$, $k_o = 3x10^9\ \mathrm{min}^{-1}$, $E/R = 8{,}330.1\,\mathrm{K}$, $-\Delta H_{rxn} = 3x10^7\ \mathrm{cal/kmol}$, $\rho = 10^6\ \mathrm{g/m}^3$, $UA = 5.34x10^6\ \mathrm{cal/K}$, $C_p = 1\,\mathrm{cal/(gK)}$, $T_S = 394\,\mathrm{K}$ and $C_{AS} = 0.265\,\mathrm{kmol/m}^3$. The state constraint is $x \in \mathbb{X}$ where $\mathbb{X} := \{x \in \mathbb{R}^2 \,|\, [1\ 0]x \le 0.08\,\mathrm{kmol/m}^3,\ \ [0\ 1]x \le 1\,\mathrm{K}\}$. The control constraint is $u \in \mathbb{U}$ where $\mathbb{U} := \{u \in \mathbb{R} \,|\, |u| \le 0.5\,\mathrm{m}^3/\mathrm{min}\}$. The disturbance and measurement noise are bounded $(w, v) \in \mathbb{W}\, x\, \mathbb{V}$ where $\mathbb{W} := \{w \in \mathbb{R}^2 \,|\, \|w\|_\infty \le 0.01\}$ and $\mathbb{V} := \{v \in \mathbb{R}^2 \,|\, \|v\|_\infty \le 0.01\}$.The discrete-time model can be obtained by discretizing (4.4) with a sampling time of 0.15 min. The state is unmeasurable so the objective is to regulate the observer state in such a way that the state of the nominal system is driven to the target set. The difference between the observer state and the state of the nominal system $e = \hat{x} - \bar{x}$ is bounded by the invariant tubes for the control error. The difference between the real state and the observer state $\tilde{x} = x - \hat{x}$ is bounded by the invariant tubes for the state estimation error.

Figure 4.7 shows the closed-loop responses of the systems. The invariant tubes for the state estimation error $\widetilde{S}_i$ and the control error $\overline{S}_i$ are shown in cyan and green,

respectively. The yellow, red and blue lines represent the state trajectories of the uncertain system, the observer system and the nominal system, respectively. The target sets $\overline{X}_f$, $\overline{X}_f \oplus \overline{S}_i$ and $\overline{X}_f \oplus \overline{S}_i \oplus \widetilde{S}_i$ are shown in blue, red and yellow, respectively. The infeasible region for the state constraint is shown in magenta. Starting from an initial observer state $\hat{x} = (-0.3, -1)$, it is seen that the state of the nominal system, the observer state and the real state are steered to target sets $\overline{X}_f$, $\overline{X}_f \oplus \overline{S}_i$ and $\overline{X}_f \oplus \overline{S}_i \oplus \widetilde{S}_i$, respectively.

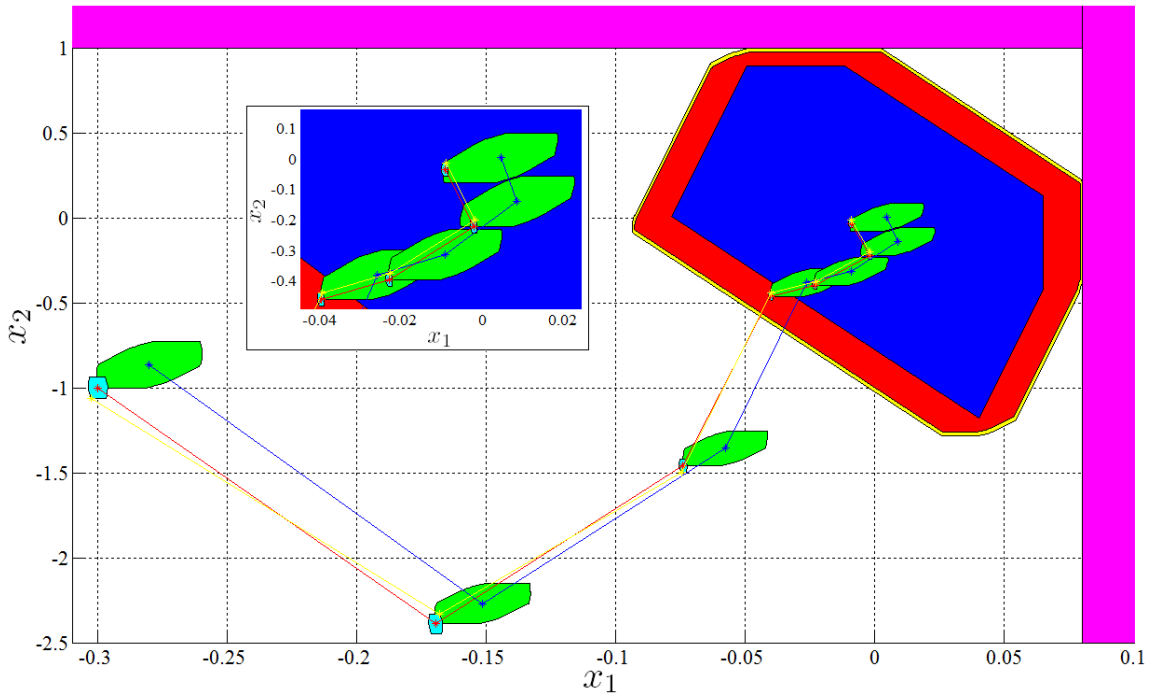

Figure 4.7 The closed-loop responses of the systems in case study 1.2. The invariant tubes for the state estimation error $\widetilde{S}_i$ and the control error $\overline{S}_i$ are shown in cyan and green, respectively. The yellow, red and blue lines represent the state trajectories of the uncertain system, the observer system and the nominal system, respectively. The target sets $\overline{X}_f$, $\overline{X}_f \oplus \overline{S}_i$ and $\overline{X}_f \oplus \overline{S}_i \oplus \widetilde{S}_i$ are shown in blue, red and yellow, respectively. The infeasible region for the state constraint is shown in magenta.

(2) Results from the development of a pilot-scale fluidized bed reactor for low-density polyethylene (LDPE)

Figure 4.8 shows the process flow diagram of a pilot-scale fluidized bed reactor. The experimental apparatus consist of the compressor, rotary valve, electric air cooler, particle feeder, fluidization chamber, heater, microelectronic controller, cyclone and filter. The compressor delivers a maximum air flow rate of 0.25 m^3/s and a maximum pressure of 1.83 bars (absolute). The air flow rate can be adjusted with a rotary valve. The air enters the fluidization chamber with a diameter of 0.15 m and the height of 1.2 m. The top section of the fluidization chamber is a dome in order to reduce possible risk of particle entrainment out of the reactor.

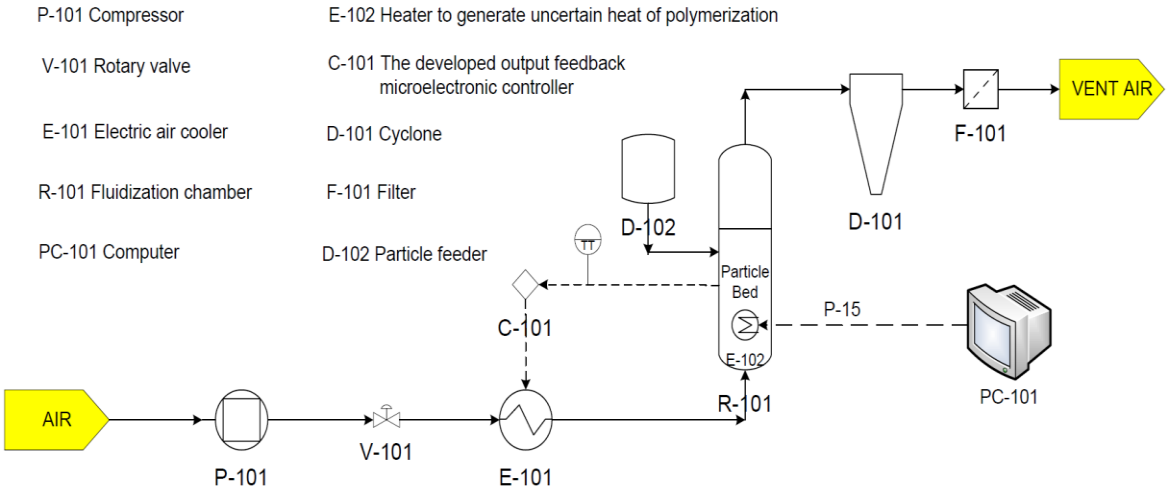

Figure 4.8 The process flow diagram of a pilot-scale fluidized bed reactor.

The compressor and the fluidization chamber in a pilot-scale fluidized bed reactor for LDPE are shown in Fig. 4.9.

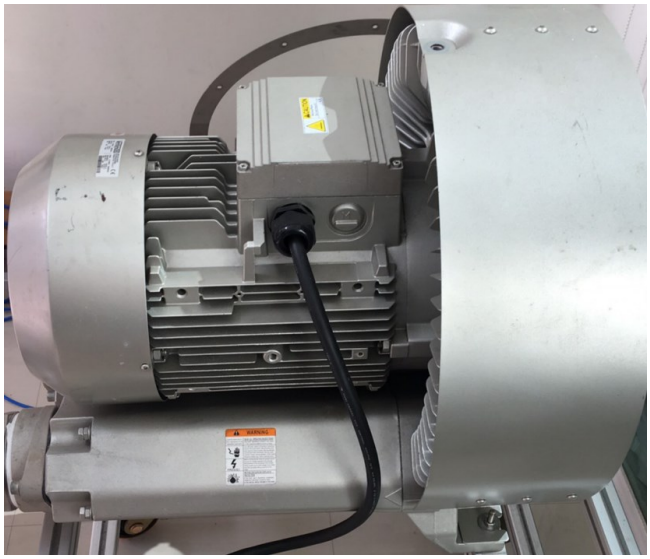

a) Compressor

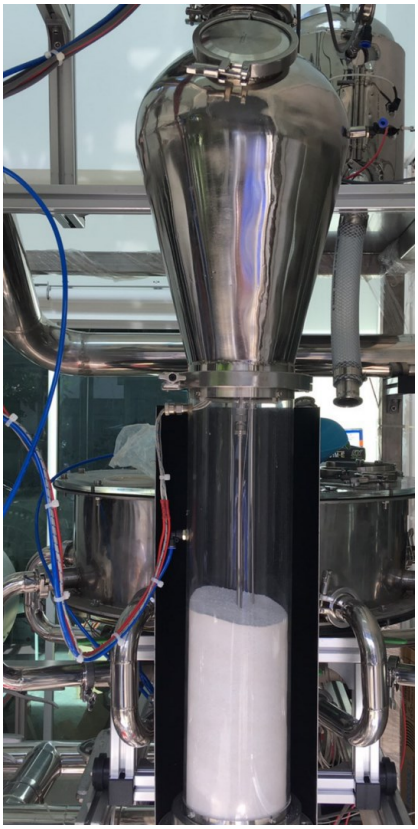

b) Fluidization chamber

Figure 4.9 a) The compressor and b) the fluidization chamber in a pilot-scale fluidized bed reactor.

The process specifications can be summarized as shown in Table 4.2.

Table 4.2 The process specifications of a pilot-scale fluidized bed reactor.

Parameter	Value	Unit
Air feed rate	max 0.25	m^3/s
Average diameter of LDPE particle	1,000	micrometer
Fluidization chamber diameter	0.15	m
Fluidization chamber height	1.2	m
Operating bed temperature	70	^oC
Operating pressure of fluidization chamber	1	bar

(3) Results from the application of the developed controller to the control of a pilot-scale fluidized bed reactor for LDPE.

In this section, the developed robust model predictive control algorithm is applied to the control of a pilot-scale fluidized bed reactor for low-density polyethylene (LDPE). The LDPE particles are loaded into the chamber that generates heat in the bed of particles according to the rate law of polymerization calculated by the computer. The objective is to regulate the temperature of the system to the set point under the influences of uncertainties such as the reaction rate constant, heat of reaction, disturbances and measurement noises.

Case study 3.1: The control performance when the reaction rate constant is uncertain.

In this case study, the developed controller is applied to the system as the reaction rate constant is uncertain. The values of the reaction rate constant are in the range between -20% to +20% from the nominal value. Figure 4.10 shows the closed-loop trajectories of the system. The developed controller can regulate the system to the set point despite the uncertain reaction rate constant. It can be observed that larger value of reaction rate constant leads to lower reactant concentration and higher temperature of the system.

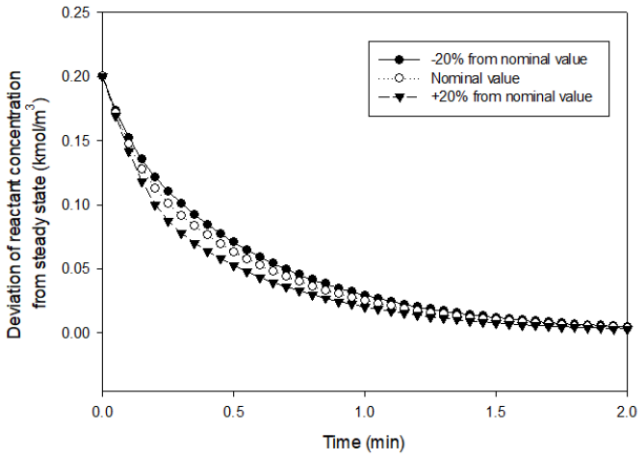

(a) reactant concentration

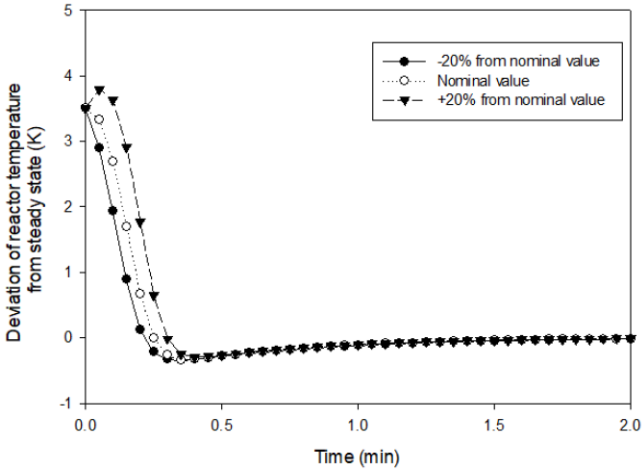

(b) reactor temperature

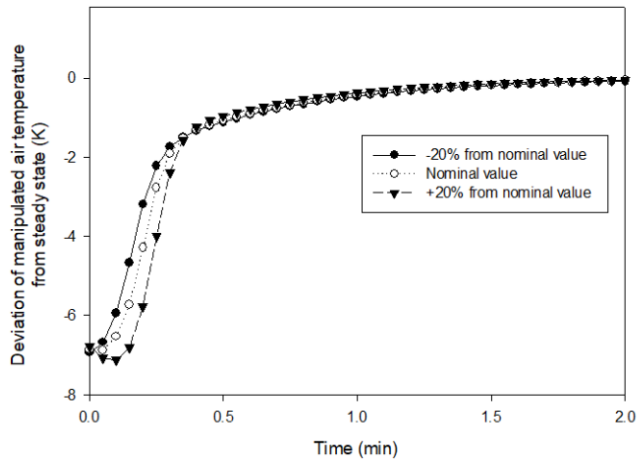

(c) manipulated air temperature

Figure 4.10 The closed-loop trajectories of the system as the reaction rate constant is uncertain.

Case study 3.2: The control performance when the heat of reaction is uncertain.

The developed controller is applied to the system as the heat of reaction is uncertain in this case study. The values of the heat of reaction are in the range between -20% to +20% from the nominal value. Figure 4.11 shows the closed-loop trajectories of the system. For high value of the heat of reaction, the overshoot of the temperature can occur in the system. This action leads to lower value of manipulated air temperature in order to reduce the temperature of the system.

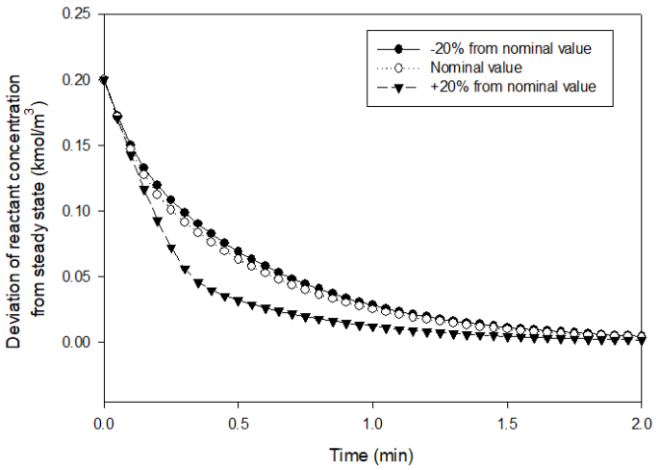

(a) reactant concentration

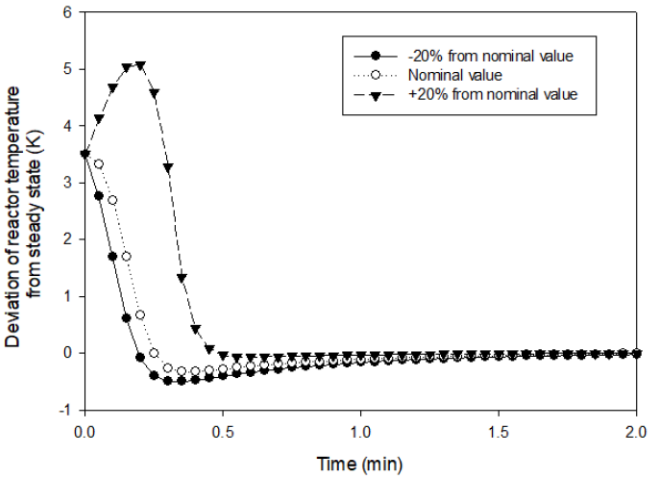

(b) reactor temperature

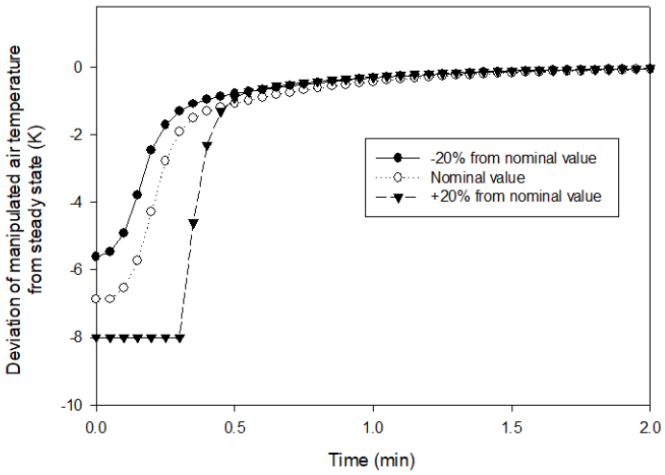

(c) manipulated air temperature

Figure 4.11 The closed-loop trajectories of the system as the heat of reaction is uncertain.

Case study 3.3: The control performance when the bed temperature measurement contains noises.

In this case study, the developed controller is applied to the system as the bed temperature measurement contains noises. The values of the bed temperature measurement noises are in the range between -2% to +2% from the nominal value. Figure 4.12 shows the closed-loop trajectories of the system. The system can be regulated to the set point despite the presence of the bed temperature measurement noises.

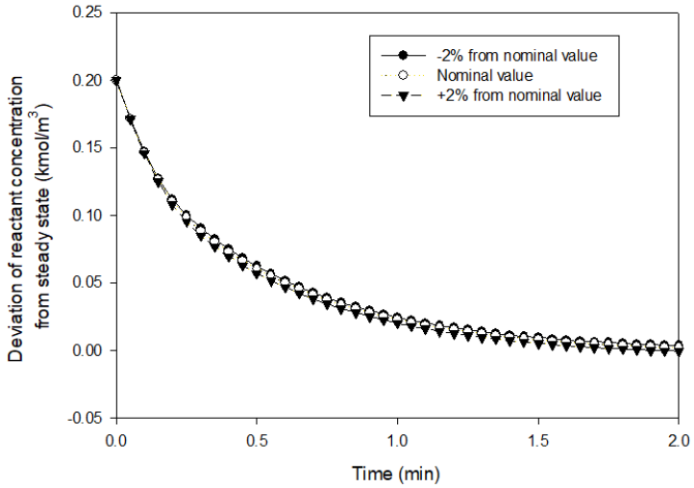

(a) reactant concentration

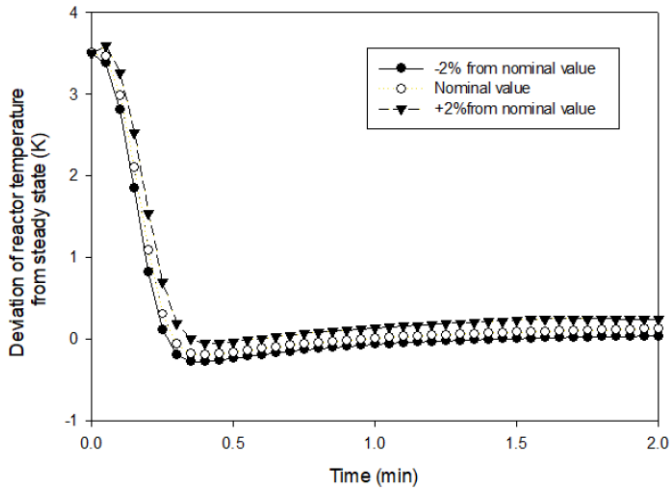

(b) reactor temperature

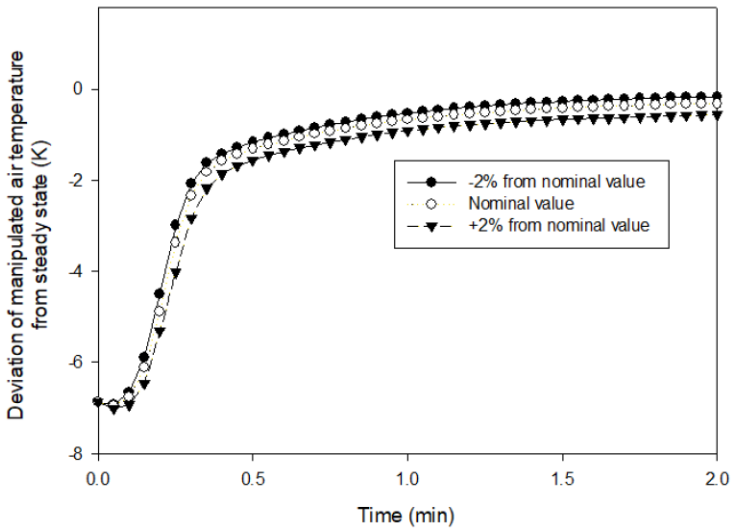

(c) manipulated air temperature

Figure 4.12 The closed-loop trajectories of the system as the bed temperature measurement contains noises.

Case study 3.4: The control performance when the inlet air temperature contains disturbances.

In this case study, the developed controller is applied to the system as the inlet air temperature contains disturbances. The values of the inlet air temperature disturbances are in the range between -2% to +2% from the nominal value. Figure 4.13 shows the closed-loop trajectories of the system. The deviation of temperature from the steady state is high as the values of disturbances increase. The temperature can be regulated to the neighborhood of the steady state as the values of disturbances increase so robust stability of the system can be guaranteed.

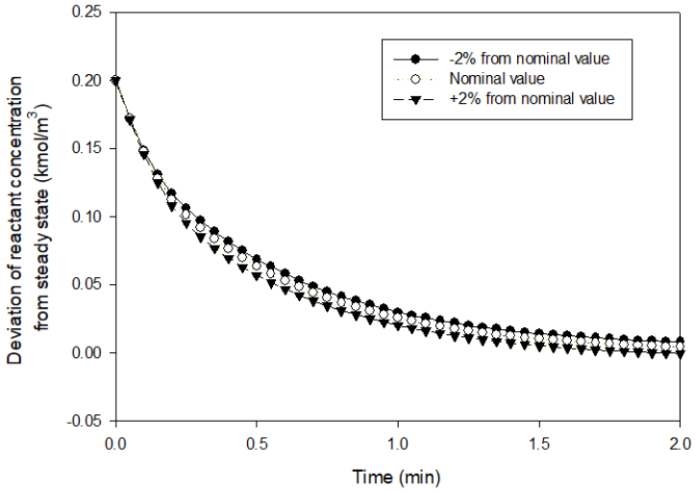

(a) reactant concentration

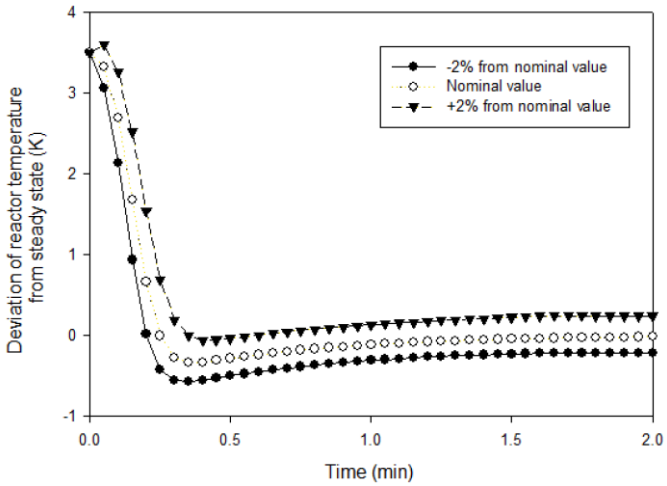

(b) reactor temperature

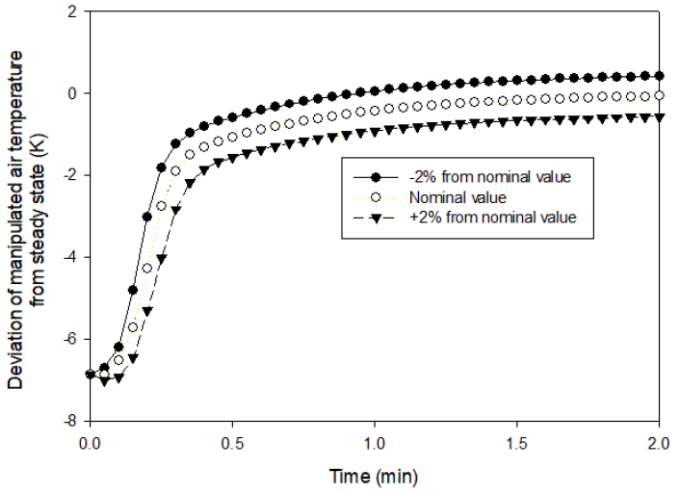

(c) manipulated air temperature

Figure 4.13 The closed-loop trajectories of the system as the inlet air temperature contains disturbances.

5. Conclusions

The control of the system in the presence of various sources of uncertainties including the uncertain parameters, disturbances and measurement noises is a challenging control problem because it is difficult to ensure both robust stability and constraint satisfaction. In this research, a novel off-line output feedback tube-based robust model predictive control algorithm is presented. The effects of the state estimation errors and all possible sources of uncertainties are bounded within the tubes so robust stability and constraint satisfaction can be guaranteed. All optimization problems are solved off-line to find the explicit control laws so the developed control algorithm can be applied to the fast dynamical systems. In order to demonstrate the effectiveness of the developed controller, it is applied to a pilot-scale fluidized bed reactor for low-density polyethylene (LDPE). The LDPE particles are loaded into the pilot-scale fluidized bed reactor and the heat within the bed is generated according to the uncertain rate of reaction simulated from the computer. The polymerization reaction is highly exothermic so it is important to control the bed temperature at the set point. The temperature measurement noises usually exist due to the fluctuating behavior of fluidization. In the presence of uncertainties including the reaction rate constant, heat of reaction, disturbances and measurement noises, the developed robust model predictive control algorithm can regulate the temperature of the system to the set point so robust stability can be guaranteed.

References

Chen, X. Z., Luo, Z. H., Yan, W. C., Lu, Y. H., and Ng, I. S. (2011). Three-dimensional CFD-PBM coupled model of the temperature fields in fluidized-bed polymerization reactors. AIChE J., 57, pp. 3351-3366.

Kvasnica, M., Grieder, P., Baotić, M., and Morari, M. (2004). Multi-Parametric Toolbox (MPT). Hybrid Systems: Computation and control, 2993, pp. 448-462.

Li, Z., Annaland, M.V.S., Kuipers, J.A.M., and Deen, N.G. (2016) Effect of superficial gas velocity on the particle temperature distribution in a fluidized bed with heat production. Chem. Eng. Sci., 140, pp. 279-290.

Mayne, D.Q., Raković, S.V., Findeisen, R., Allgöwer, F. (2006). Robust output feedback model predictive control of constrained linear systems. Automatica, 42, pp. 1217-1222.

Mayne, D.Q., Raković, S.V., Findeisen, R., Allgöwer, F. (2009). Robust output feedback model predictive control of constrained linear systems: Time varying case. Automatica, 45, pp. 2082-2087.

Raković, S.V., Kerrigan, E.C., Kouramas, K.I., and Mayne, D.Q. (2005). Invariant approximations of the minimal robust positively invariant set. IEEE T. Automat. Contr., 50, pp. 406-410.

Schneiderbauer, S., Puttinger, S., Pirker, S., Aguayo, P., and Kanellopoulos, V. (2015). CFD modeling and simulation of industrial scale olefin polymerization fluidized bed reactors. Chem. Eng. J., 264, pp. 99-112.

Wan, Z., and Kothare, M.V. (2002). Robust output feedback model predictive control using off-line linear matrix inequalities. J. Process Contr., 12, pp. 763-774.

6. Recommendations for future research

6.1 The range of the uncertainties in this work may be limited due to some constraints and limitations of the system. Future work can be extended to accommodate more values of uncertainties.

6.2 As the economic performance is important for the industrial process, the economic model predictive control involving the costs and profits can be developed in the future work.

7. Outputs of this research

7.1 ผลงานตีพิมพ์ในวารสารวิชาการนานาชาติ

1) Kusolsongtawee, T., and Bumroongsri, P. (2018). Two-stage modeling strategy for industrial fluidized bed reactors in gas-phase ethylene polymerization processes. Chemical Engineering Research and Design, 140, pp. 68-81. Impact Factor 3.073

2) Yadbantung, R., and Bumroongsri, P. (2019). Tube-based robust output feedback MPC for constrained LTV systems with applications in chemical processes. European Journal of Control, 47, pp. 11-19. Impact Factor 1.549

7.2 การนำผลงานวิจัยไปใช้ประโยชน์

1) เชิงสาธารณะ โดยสถาบันการศึกษา
งานวิจัยที่เกิดขึ้นส่งเสริมให้เกิดการสร้างเครือข่ายความร่วมมือในการวิจัยระหว่างอาจารย์ต่างมหาวิทยาลัยที่ทำงานวิจัยในกลุ่มเดียวกัน ซึ่งประกอบด้วย

1. รศ.ดร.สุรเทพ เขียวหอม
ภาควิชาวิศวกรรมเคมี คณะวิศวกรรมศาสตร์ จุฬาลงกรณ์มหาวิทยาลัย
2. ผศ.ดร.อมรชัย อาภรณ์วิชานพ
ภาควิชาวิศวกรรมเคมี คณะวิศวกรรมศาสตร์ จุฬาลงกรณ์มหาวิทยาลัย
3. ผศ.ดร.วีรยุทธ เลิศบำรุงสุข
ภาควิชาวิศวกรรมเคมี คณะวิศวกรรมศาสตร์และเทคโนโลยีอุตสาหกรรม มหาวิทยาลัยศิลปากร
4. ผศ.ดร.พรชัย บำรุงศรี
ภาควิชาวิศวกรรมเคมี คณะวิศวกรรมศาสตร์ มหาวิทยาลัยมหิดล

2) เชิงวิชาการ โดยภาควิชาวิศวกรรมเคมี คณะวิศวกรรมศาสตร์ มหาวิทยาลัยมหิดล
งานวิจัยนี้ก่อให้เกิดองค์ความรู้ใหม่ซึ่งนำไปใช้ในการพัฒนาการเรียนการสอนโดยการเป็นวิทยากรบรรยายพิเศษรายวิชา EGCH 691 Seminar ซึ่งเป็นรายวิชาของนักศึกษาในระดับบัณฑิตศึกษา (นานาชาติ) ของคณะวิศวกรรมศาสตร์ มหาวิทยาลัยมหิดล

7.3 อื่นๆ

1) งานวิจัยนี้ก่อให้เกิดองค์ความรู้ใหม่ซึ่งได้รับเชิญเป็น speaker ณ. คณะวิศวกรรมศาสตร์ จุฬาลงกรณ์มหาวิทยาลัย สำหรับผลงานวิจัยเรื่อง
Yadbantung, R., Kheawhom, S., and Bumroongsri, P. (2019). Nonlinear model predictive control of chemical reactors with uncertain economic costs, The 8th International Symposium on Design, Operation and Control of Chemical Processes (PSE Asia 2019), January 13-16, Chulalongkorn University, Bangkok, Thailand.

2) โครงการวิจัยก่อให้เกิดความร่วมมือจากภาคส่วนต่างๆดังตัวอย่างงานวิจัย
Duangsri, S., Kheawhom, S., and Bumroongsri, P. (2019). A PDE-based data reconciliation approach for systems with variations of parameters. Engineering Jouirnal, 23, pp. 157-169. (Scopus Q2)

Appendix

แนบผลงานตีพิมพ์ในวารสารวิชาการนานาชาติ